



UNIVERSITY
OF WOLLONGONG
AUSTRALIA

University of Wollongong
Research Online

Faculty of Engineering - Papers (Archive)

Faculty of Engineering and Information Sciences

2011

Continuously tunable magnetic phase transitions in the DyMn_{1-x}Fe_xO₃ system

Fang Hong

fh640@uowmail.edu.au

Zhenxiang Cheng

University of Wollongong, cheng@uow.edu.au

Hongyang Zhao

National Institute Materials Science, Japan

Hideo Kimura

National Institute For Materials Science

Xiaolin Wang

University of Wollongong, xiaolin@uow.edu.au

<http://ro.uow.edu.au/engpapers/3883>

Publication Details

Hong, F., Cheng, Z., Zhao, H., Kimura, H. and Wang, X. (2011). Continuously tunable magnetic phase transitions in the DyMn_{1-x}Fe_xO₃ system. Applied Physics Letters, 99 (9), 092502-1-092502-3.

Research Online is the open access institutional repository for the University of Wollongong. For further information contact the UOW Library: research-pubs@uow.edu.au

Continuously tunable magnetic phase transitions in the $\text{DyMn}_{1-x}\text{Fe}_x\text{O}_3$ system

Fang Hong, Zhenxiang Cheng, Hongyang Zhao, Hideo Kimura, and Xiaolin Wang

Citation: *Appl. Phys. Lett.* **99**, 092502 (2011); doi: 10.1063/1.3632061

View online: <http://dx.doi.org/10.1063/1.3632061>

View Table of Contents: <http://apl.aip.org/resource/1/APPLAB/v99/i9>

Published by the American Institute of Physics.

Related Articles

Transition from paramagnetism to ferromagnetism in HfO_2 nanorods

J. Appl. Phys. **113**, 076102 (2013)

The competing spin orders and fractional magnetization plateaus of the classical Heisenberg model on Shastry-Sutherland lattice: Consequence of long-range interactions

J. Appl. Phys. **113**, 073908 (2013)

Effect of barium-deficiency on the structural, magnetic, and magnetocaloric properties of $\text{La}_{0.6}\text{Sr}_{0.2}\text{Ba}_{0.2-x}\text{MnO}_3$ ($0 \leq x \leq 0.15$)

J. Appl. Phys. **113**, 073905 (2013)

Thermally activated magnetization switching in a nanostructured synthetic ferrimagnet

J. Appl. Phys. **113**, 063914 (2013)

Anomalous magnetoresistance and magnetocaloric properties of NdRu_2Ge_2

Appl. Phys. Lett. **102**, 062406 (2013)

Additional information on *Appl. Phys. Lett.*

Journal Homepage: <http://apl.aip.org/>

Journal Information: http://apl.aip.org/about/about_the_journal

Top downloads: http://apl.aip.org/features/most_downloaded

Information for Authors: <http://apl.aip.org/authors>

ADVERTISEMENT

AIP | Applied Physics
Letters

EXPLORE WHAT'S NEW IN APL

SUBMIT YOUR PAPER NOW!

SURFACES AND INTERFACES
Focusing on physical, chemical, biological, structural, optical, magnetic and electrical properties of surfaces and interfaces, and more...

ENERGY CONVERSION AND STORAGE
Focusing on all aspects of static and dynamic energy conversion, energy storage, photovoltaics, solar fuels, batteries, capacitors, thermoelectrics, and more...

Continuously tunable magnetic phase transitions in the $\text{DyMn}_{1-x}\text{Fe}_x\text{O}_3$ system

Fang Hong,¹ Zhenxiang Cheng,^{1,a)} Hongyang Zhao,² Hideo Kimura,² and Xiaolin Wang¹

¹Institute for Superconducting and Electronic Materials, University of Wollongong, New South Wales 2519, Australia

²National Institute for Materials Science, 1-2-1 Sengen, Tsukuba, Japan

(Received 16 June 2011; accepted 5 August 2011; published online 29 August 2011)

The structure and magnetic properties of perovskite $\text{DyMn}_{1-x}\text{Fe}_x\text{O}_3$ samples have been studied. Static orbital orderings are expected to exist in samples with $x \leq 0.2$ due to strong Jahn-Teller distortion, which become less stable as x increases and probably disappears in samples with $x > 0.5$. The antiferromagnetic transition temperature increases as x increases. At the composition $x > 0.5$, spin reorientation starts to appear. Meanwhile, the spin reorientation temperature and the antiferromagnetic Néel temperature gradually separate and widen the temperature range of the magnetic metastable state between these two transitions. The magnetic competition is discussed based on exchange interaction and Dzyaloshinsky-Moriya interaction. © 2011 American Institute of Physics. [doi:10.1063/1.3632061]

Multiferroic materials are potential functional materials for future spintronic application.^{1,2} A great amount of work has been done to explore mutual control of the electric and magnetic degrees of freedoms, the so-called magnetoelectric (ME) coupling.^{3–5} Meanwhile, the abundant phase transitions that occur in some multiferroic systems have inspired great interest.^{6,7} The dielectric property changes around the magnetic phase transition can offer a way to achieve magnetodielectric coupling. One can modify the magnetic transition and the dielectric property by an external magnetic field.^{8–11} Magnetic competition in some rare earth manganites, such as orthorhombic TbMnO_3 (Ref. 7) and GdMnO_3 ,⁷ as well as DyMnO_3 ,^{7,12,13} could induce magnetic frustration and complex spin states. Cross-coupling between ferroelectricity and magnetism can be realized in these manganites because of the broken spatial inversion and time-reversal symmetries.¹⁴

In rare earth orthoferrites, a special magnetic phase transition occurs, called spin reorientation. A representative example of this kind of material is DyFeO_3 .^{8,15,16} It is the only rare-earth orthoferrite to show Morin transition, where the Fe^{3+} system spins in single crystal reorient from $\Gamma 4$ (antiferromagnetic (AFM) configuration along a axis with weak ferromagnetic (WFM) component along c axis) to $\Gamma 1$ (simple un-canted antiferromagnetism along b axis) around 35 K.¹⁷ Much more interesting, Tokunaga and Tokura *et al.* found that the magnetic field along c axis of DyFeO_3 single crystal ($Pbnm$) can induce a gigantic ME effect.¹⁸ In addition, Kimel *et al.* reported that they had achieved spin reorientation in TmFeO_3 via ultra-short laser pulses.¹⁹ Considering the possible control of magnetic anisotropy by lattice strain, these materials are possible choices to achieve ME coupling if they are combined with ferroelectric materials.

At present, spintronic application has to meet many challenges, and one may be finding strong ME coupling at room temperature in multiferroic materials. The core of this challenge is the modification of magnetic and electric polarization phases. Therefore, phase transition research becomes extremely important and can give us theoretical and experimental guidance in the search for multiferroic materials. In this letter, we study the spin reorientations and antiferromagnetic transitions in the distorted perovskite $\text{DyMn}_{1-x}\text{Fe}_x\text{O}_3$ system. The results show something of interest and suggest a possible way to achieve ME coupling and modify multiferroic properties in this type of material.

Polycrystalline samples of $\text{DyMn}_{1-x}\text{Fe}_x\text{O}_3$ ($x = 0, 0.2, 0.33, 0.5, 0.6, 0.67, 0.8, 0.95, \text{ and } 1.0$) were made by the solid state reaction method. Stoichiometric amounts of raw oxide powder were weighed carefully and mixed in an agate mortar, followed by pressing into pellets 15 mm in diameter at 20 MPa. Samples were calcined at 950 °C for 10 h and sintered at 1440 °C for 6 h. The crystal structures of the samples were examined by x-ray diffraction (XRD, model: GBC Mini-Materials Analyzer) at room temperature. The magnetic measurements and the heat capacity were carried out using a 14 T physical properties measurement system (PPMS).

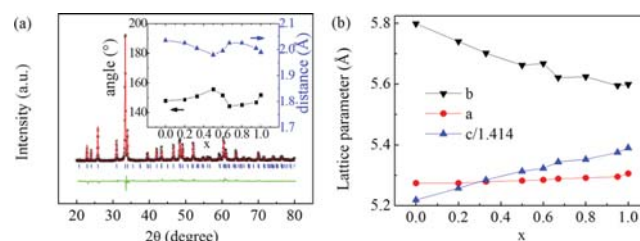


FIG. 1. (Color online) (a) XRD refinement calculation results on $\text{DyMn}_{0.8}\text{Fe}_{0.2}\text{O}_3$ with $R_p = 8.9\%$ (star symbols, experiment data; solid line, fitting data; short vertical solid lines, Bragg positions; fluctuation line at bottom, difference). Inset: Fe content dependence of Mn/Fe-O-Mn/Fe angles and Mn/Fe-O distances within ab -plane. (b) Lattice parameter dependence on Fe content.

^{a)}Author to whom correspondence should be addressed. Electronic mail: cheng@uow.edu.au.

Fig. 1(a) shows the typical results of Rietveld structural refinement of $\text{DyMn}_{0.8}\text{Fe}_{0.2}\text{O}_3$ with R_p value of 8.9%. All diffraction patterns can be assigned to the single phase orthorhombic structure with space group $Pbnm$. The Fe content dependence of average Mn/Fe-O bonding distances and Mn/Fe-O-Mn/Fe angles within ab -plane are given in the inset. There are two transitions at $x = 0.5$ and $x = 0.67$, suggesting two magnetic transitions. The lattice parameter dependence on the Fe content is shown in Fig. 1(b). With increasing x , both a axis and c axis become longer monotonously, while b axis decreases linearly but shows weak fluctuation above $x = 0.5$.

The measurement of the field and zero-field cooling (FC and ZFC) temperature dependence of the magnetic moment was carried out for samples with $0 \leq x \leq 0.5$. DyMnO_3 shows a typical paramagnetic (PM)-like state over the whole temperature range, as seen in Fig. 2(a). It was reported that DyMnO_3 changes to an AFM state around 39 K.^{7,13} Because of the strongly paramagnetic Dy^{3+} , the transition from PM state to AFM state is masked. However, the heat capacity measurement confirmed this magnetic phase transition and Dy^{3+} ordering around 6.5 K (shown in supplement files, Fig. S1 (Ref. 25)). When the Fe content increases, the ZFC and FC curves separate from each other at higher temperature, suggesting a possible magnetic phase transition (shown in supplement files, Fig. S2 (Ref. 25)). To remove the Dy^{3+} moment contribution and determine the exact phase transition temperature, we plot the normalized $d\gamma/dT$ -T curves (shifted by proper interval), as shown in the inset of Fig. 2(a). Clear peaks can be observed and the magnetic phase transition temperature increases when the Fe content increases.

Low temperature and high temperature FC magnetic properties for samples with $0.5 < x \leq 1$ were measured on heating in a field of 1000 Oe, as shown in Figs. 2(b) and 2(c), respectively. There are two transitions which correspond to the sudden change of magnetic moment. The spin

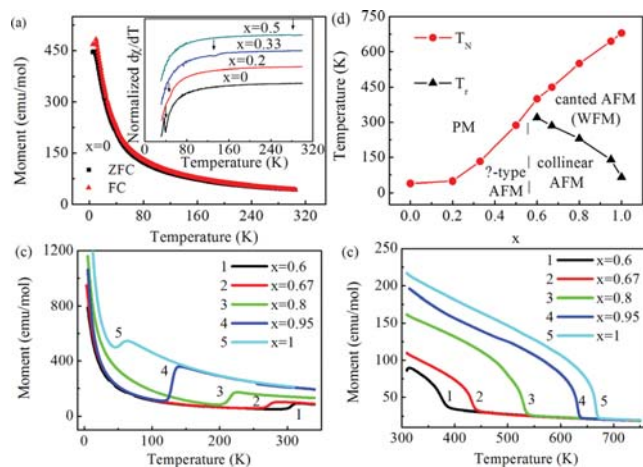


FIG. 2. (Color online) (a) ZFC and FC M-T curves of DyMnO_3 . Inset: Temperature dependence of normalized $d\gamma/dT$ for $x \leq 0.5$. (b) and (c) Temperature dependence of magnetic moment at low/high temperature range for $0.5 < x \leq 1$. (d) The Fe content dependence of the Néel temperatures (T_N) and spin reorientation temperatures (T_r). Speculated magnetic states are presented.

state of Fe^{3+} and Mn^{3+} can be obtained by Curie Weiss Law fitting (shown in supplement files, Fig. S3 (Ref. 25)). For the rare earth metal ion Dy^{3+} , its maximum effective moment is $9.9 \mu_B/\text{at.}$ found in the oxide state. Fitting results show that all values of the Dy^{3+} effective moment are above $9.5 \mu_B/\text{at.}$, if Fe^{3+} and Mn^{3+} are in high spin state ($\text{Fe}^{3+}:S = 5/2$, $5.9 \mu_B/\text{at.}$ and $\text{Mn}^{3+}:S = 2$, $4.9 \mu_B/\text{at.}$), indicating that Fe^{3+} and Mn^{3+} must always be in high spin state, no matter what the Fe content. In addition, all Curie Weiss Law fittings give negative Curie-Weiss temperatures. Negative Curie Weiss temperatures indicate that the transitions at high temperature range are AFM transitions. The high spin states of Mn^{3+} and Fe^{3+} further confirm that they are AFM transitions rather than ferromagnetic (FM) transitions. The increasing moment below this transition indicates that the AFM states are not pure but with WFM component. The existence of FM clusters can be easily excluded because the magnetic hysteresis loop measured at 5 K shows typical PM/AFM behaviour presented in Fig. 3(b). Hence, the high temperature transitions are transitions from PM states to canted AFM states. The sudden decrease of magnetic moment at low temperature in Fig. 2(b) should be the result of disappearance of WFM component. Hence, the transition at low temperature range is assigned to spin reorientation from canted AFM state to collinear AFM state. The spin reorientation temperature shifts to lower temperature with increasing Fe content while T_N increases. The Fe content dependence of all transition temperatures is presented in Fig. 2(d). Hence, the two transitions of bonding distances and angles within ab -plane just reflect the Fe doping induced magnetic transitions from paramagnetic state ($0 \leq x \leq 0.5$) to collinear antiferromagnetic state ($x = 0.6$) to canted antiferromagnetic state ($0.67 \leq x \leq 1$) at room temperature.

In distorted perovskite ABO_3 type compounds with orthorhombic structure, such as LaMnO_3 (Ref. 20) and YbMnO_3 ,²¹ the cooperative rotation of corner-sharing BO_6 octahedra can bias the cooperative Jahn-Teller orbital ordering. In-plane magnetic interaction of BO_6 octahedra is decided by the competition between the FM interaction of e_g electrons (σ -bond component) and the AFM interaction of t_{2g} electrons (π -bond component). The interplane magnetic interaction can be divided into two major parts, according to the different contributions from electrons in different 3d sub-orbitals. One is the AFM interaction between the half-filled t_{2g} orbitals of transition metal B ions via O^{2-} ions. The other is the AFM and FM competition interaction among e_g orbitals (e.g., $3z^2-r^2$ and x^2-y^2). Generally, the interplane AFM interaction of t_{2g} plays a dominating role, resulting in an

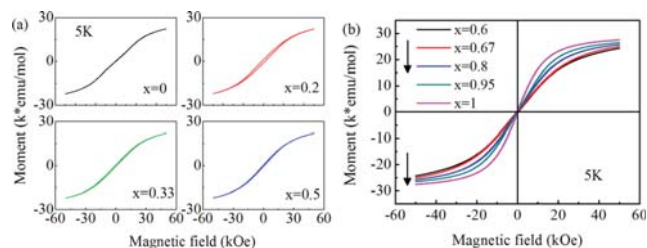


FIG. 3. (Color online) Magnetic hysteresis loops at 5 K from -5 T to 5 T for samples with (a) $x \leq 0.5$ and (b) $0.5 < x \leq 1$.

AFM spin configuration along c axis. For LaMnO_3 , there is an A-type antiferromagnetic order due to the dominating FM interaction of e_g in-plane.²⁰ Here, DyMnO_3 shows an incommensurate antiferromagnetic configuration with a wave number of 0.72 at T_N .^{7,13} Our experiment shows that the AFM transition temperatures of $\text{DyMn}_{1-x}\text{Fe}_x\text{O}_3$ are modified by Fe doping, which stems from subtle structural change. For DyMnO_3 and low Fe doping samples with $x \leq 0.2$, a relation $b > a > c/\sqrt{2}$ is found, suggesting a static Jahn-Teller orbital ordering. Therefore, for $x \leq 0.5$, the Fe doping can affect the magnetic exchange interaction in the following way: because e_g orbital of Fe^{3+} ion is half occupied and that of Mn^{3+} ion is quarter occupied, such an occupied electronic state enhances the AFM exchange interaction of the whole system, both in-plane and interplane, according to the Hund rule. In addition, Fe doping also promotes the increase in $c/\sqrt{2}$ relative to a , the orbital ordering becomes less stable and stronger AFM interaction of $e_g^2\text{-O}-e_g^2$ (Fe-O-Fe) emerges. The increasing Mn/Fe-O-Mn/Fe angles within ab -plane confirm the enhancement of AFM interaction according to the Goodenough-Kanamori (GK) rule.²²⁻²⁴ For $x > 0.5$, the magnetic interaction should be considered in a quite different way. Similar to $\text{Yb}(\text{Mn}_{1-x}\text{Fe}_x)\text{O}_3$,²¹ despite the disappearance of the static Jahn-Teller distortion and long range orbital order, the dynamic Jahn-Teller site transformation still remains. The AFM interaction totally overwhelms the weak FM interaction of electrons in the Mn^{3+} e_g orbital and favours the G-type spin configuration. Moreover, this AFM interaction becomes much stronger in samples with higher Fe doping level so that T_N shifts significantly. In G-type antiferromagnetic order, a weak FM component could be induced along c axis because of Dzyaloshinsky-Moriya (DM) interaction, if spins are normal to b axis in ab -plane.²¹ This is in accordance with the observed weak FM transition in our experiment.

As for spin reorientation, there are a few factors that affect this transition: magnetic anisotropy, single ion anisotropy, the DM interaction, and exchange interaction. In our case, $\text{Dy}^{3+}\text{-Fe}^{3+}/\text{Mn}^{3+}$ ion exchange interaction seems to play an important role. In a pure DyFeO_3 sample, the spin reorientation takes place at a relatively low temperature, ~ 65 K (T_P), when the strong $\text{Dy}^{3+}\text{-Fe}^{3+}$ interaction dominates the $\text{Fe}^{3+}\text{-Fe}^{3+}$ interaction along one axis over other axis. For samples with lower Fe content, the $\text{Fe}^{3+}\text{-Fe}^{3+}$ interaction in the whole system becomes weaker because of Mn^{3+} substitution. Hence, even at higher temperature, the $\text{Dy}^{3+}\text{-Fe}^{3+}$ interaction can overwhelm thermal disturbance and the $\text{Fe}^{3+}\text{-Fe}^{3+}$ interaction, forcing spin reorientation to occur.

The M-H loops at 5 K of all samples are plotted in Fig. 3. For $x \leq 0.5$, M-H loops are shown in Fig. 3(a) individually and the saturation magnetic moments are nearly the same, but obvious remnant moments can be observed except DyMnO_3 . Remnant moments decrease when x increases. DyMnO_3 is neither the standard PM loop nor an AFM loop which should be attributed to the spiral magnetic configuration below 20 K.⁷ This indicates that Fe doping not only enhances antiferromagnetic interaction, but also induces stronger or weaker spin frustration compared with non-doped spiral DyMnO_3 , especially at low doping rates. The local DM interaction among these frustrated spins may be

responsible for the weak ferromagnetic component at low temperature. For $x > 0.5$, it is clear that the saturation magnetic moments increase when x increases and there are no remnant moments, shown in Fig. 3(b), meaning that it is collinear antiferromagnetism after spin reorientation.

In summary, we have studied polycrystalline perovskite $\text{DyMn}_{1-x}\text{Fe}_x\text{O}_3$ samples by means of structural and magnetic measurements. In samples with $x \leq 0.2$, strong Jahn-Teller distortion favours static orbital orderings, which become less stable in samples with $x \leq 0.5$ and probably disappears in samples with $x > 0.5$, according to the analysis of structure and magnetic property. Because of the introduction of Fe^{3+} , which is half-occupied in e_g orbital, the AFM transition temperatures become very sensitive to Fe content and shift to higher temperatures from 39 K to 680 K. When x exceeds 0.5, spin reorientations take place at certain temperatures which show an opposite shifting tendency to T_N .

Zhenxiang Cheng acknowledges the Australian Research Council for support through a Future Fellowship (FT 0990287).

- ¹G. Catalan and J. F. Scott, *Adv. Mater.* **21**, 2463 (2009).
- ²C. A. F. Vaz, J. Hoffman, C. H. Anh, and R. Ramesh, *Adv. Mater.* **22**, 2900 (2010).
- ³I. Fina, L. Fabrega, X. Marti, F. Sanchez, and J. Fontcuberta, *Appl. Phys. Lett.* **97**, 232905 (2010).
- ⁴V. Garcia, M. Bibes, L. Bocher, S. Valencia, F. Kronast, A. Crassous, X. Moya, S. Enouz-Vedrenne, A. Gloter, D. Imhoff, C. Deranlot, N. D. Mathur, S. Fusil, K. Bouzehouane, and A. Barthelemy, *Science* **327**, 1106 (2010).
- ⁵T. Lottermoser, T. Lonkai, U. Amann, D. Hohlwein, J. Ihringer, and M. Fiebig, *Nature* **430**, 541 (2004).
- ⁶J. Hemberger, F. Schrettle, A. Pimenov, P. Lunkenheimer, V. Y. Ivanov, A. A. Mukhin, A. M. Balbashov, and A. Loidl, *Phys. Rev. B* **75**, 035118 (2007).
- ⁷T. Kimura, G. Lawes, T. Goto, Y. Tokura, and A. P. Ramirez, *Phys. Rev. B* **71**, 224425 (2005).
- ⁸S. J. Luo, S. Z. Li, N. Zhang, T. Wei, X. W. Dong, K. F. Wang, and J. M. Liu, *Thin Solid Films* **519**, 240 (2010).
- ⁹H. M. Jang, J. H. Park, S. W. Ryu, and S. R. Shannigrahi, *Appl. Phys. Lett.* **93**, 252904 (2008).
- ¹⁰V. B. Naik and R. Mahendiran, *J. Appl. Phys.* **106**, 123910 (2009).
- ¹¹R. Muralidharan, T. H. Jang, C. H. Yang, Y. H. Jeong, and T. Y. Koo, *Appl. Phys. Lett.* **90**, 012506 (2007).
- ¹²N. Zhang, K. F. Wang, S. J. Luo, T. Wei, X. W. Dong, S. Z. Li, J. G. Wan, and J. M. Liu, *Appl. Phys. Lett.* **96**, 252902 (2010).
- ¹³T. Kimura, S. Ishihara, H. Shintani, T. Arima, K. T. Takahashi, K. Ishizaka, and Y. Tokura, *Phys. Rev. B* **68**, 060403 (2003).
- ¹⁴M. Mostovoy, *Phys. Rev. Lett.* **96**, 067601 (2006).
- ¹⁵Y. Du, Z. X. Cheng, X. L. Wang, and S. X. Dou, *J. Appl. Phys.* **107**, 09D908(2010).
- ¹⁶V. V. Eremanenko, S. L. Gnatchenko, N. F. Kharchenko, P. P. Lebedev, K. Piotrowski, H. Szymczak, and R. Szymczak, *Europhys. Lett.* **4**, 1327 (1987).
- ¹⁷L. A. Prelorendjo, C. E. Johnson, M. F. Thomas, and B. M. Wanklyn, *J. Phys. C* **13**, 2567 (1980).
- ¹⁸Y. Tokunaga, S. Iguchi, T. Arima, and Y. Tokura, *Phys. Rev. Lett.* **101**, 097205 (2008).
- ¹⁹A. V. Kimel, A. Kirilyuk, A. Tsvetkov, R. V. Pisarev, and T. Rasing, *Nature* **429**, 850 (2004).
- ²⁰I. Solovyev, N. Hamada, and K. Terakura, *Phys. Rev. Lett.* **76**, 4825 (1996).
- ²¹Y. H. Huang, M. Karppinen, N. Imamura, H. Yamauchi, and J. B. Goodenough, *Phys. Rev. B* **76**, 174405 (2007).
- ²²J. B. Goodenough, *Phys. Rev.* **100**, 564 (1955).
- ²³J. Kanamori, *J. Phys. Chem. Solids* **10**, 87 (1959).
- ²⁴J. B. Goodenough, *J. Phys. Chem. Solids* **6**, 287 (1958).
- ²⁵See supplementary material at <http://dx.doi.org/10.1063/1.3632061> for heat capacity property, ZFC-FC curves and Curie Weiss law fitting.